Organic & Biomolecular Chemistry

ROYAL SOCIETY OF CHEMISTRY

PAPER

View Article Online
View Journal | View Issue

Cite this: *Org. Biomol. Chem.*, 2023, **21**, 3214

Host–guest complexation of phthalimide-derived strigolactone mimics with cyclodextrins. Application in agriculture against parasitic weeds†

Antonio Cala Peralta, [a] Francisco J. R. Mejías, [a,b] Jesús Ayuso, [c] Carlos Rial, [a] José M. G. Molinillo, [a] José A. Álvarez, [c] Stefan Schwaiger [b] and Francisco A. Macías *[a]

Parasitic weeds are noxious plants that damage crops of economic relevance, especially in Mediterranean and African countries. The strategy of suicidal germination was proposed to deal with this plague by using seed germination inducers that work as a pre-emergence herbicide and reduce the parasitic seed load before sowing. *N*-Substituted phthalimides with a furanone ring were found to be efficient in inducing the germination of *Phelipanche ramosa* and *Orobanche cumana*, two of the most problematic parasitic weeds of crops. However, the solubility of these compounds in water is low. A strategy for enhancing their aqueous solubility is the synthesis of host–guest complexes with cyclodextrins. Three bioactive phthalimide-lactones (**PL01**, **PL04**, and **PL07**) were selected and studied to form complexes of increased water solubility with α-, β-, HP-β-, and γ-cyclodextrin. The complexes obtained by the coprecipitation method, with increased aqueous solubility (up to 3.8 times), were studied for their bioactivity and they showed similar or slightly higher bioactivity than free phthalimide-lactones, even without the addition of organic solvents. A theoretical study using semiempirical calculations of molecular models including a solvation system confirmed the physicochemical empirical results. These results demonstrated that cyclodextrins can be used to improve the physicochemical and biological properties of parasitic seed germination inducers.

Received 13th February 2023,
Accepted 21st March 2023

DOI: 10.1039/d3ob00229b

rsc.li/obc

Introduction

Strigolactones are phytohormones involved in the root/branch architecture, development and stress resistance of plants.[1–3] However, these compounds exhibit an undesired secondary role as signaling compounds for the germination of parasitic plants. Even though strigolactones are released in very small quantities into the soil (around 15 pg per plant per day),[4] this amount is high enough to initiate the life cycle of parasitic plants. This is the case for the seeds of the genera *Orobanche*, *Phelipanche*, and *Striga*, which start germination by recognizing concentrations as low as 10^{-12} M.[5] Parasitic plants are a serious problem, causing crop losses amounting to billions of dollars around the world and, especially, in Africa and Mediterranean countries.[6] In the case of obligate parasites, a suicidal germination strategy (recently, also named honeypot strategy[7,8]) was proposed to deal with these weeds, where a low concentration of strigolactones can be employed as pre-emergence treatment of the soil before the cultivation of crops to cause the death of parasitic plants by starvation.[9]

Stability and availability are the two major problems associated with the practical application of the aforementioned strategy. The isolation of strigolactones from natural sources provides a very low yield and takes a lot of effort, making it impractical for large scale purposes. For example, up to 0.35 mg and 0.15 mg of (+)-2′-*epi*-orobanchol and (+)-orobanchol, respectively, can be isolated from 5000 seedlings of 5-month grown tobacco plants.[10] Strigolactones like solanacol or solanacyl acetate are fully degraded after 4 to 9 days in water, and only 50% remain after 2 to 4 days, respectively.[11]

In order to successfully apply the suicidal germination strategy, strigolactone mimics with better stability and low cost have been proposed. More than 15 synthesis steps have to be performed to obtain low amounts of nature identical strigolac-

[a]*Department of Organic Chemistry, Institute of Biomolecules (INBIO), University of Cádiz, República Saharaui 7, 11510 Puerto Real, Cádiz, Spain.*
E-mail: famacias@uca.es
[b]*Institute of Pharmacy/Pharmacognosy, Center for Molecular Biosciences Innsbruck CMBI, University of Innsbruck, Innrain 80-82, A-6020 Innsbruck, Austria*
[c]*Physical Chemistry Department, Institute of Biomolecules (INBIO), Campus CEIA3, School of Science, University of Cadiz, C/Republica Saharaui 7, Puerto Real, Cádiz, 11510, Spain*

†Electronic supplementary information (ESI) available: Images of the geometrically optimized models for the least stable optimizations and high quality images of the stable complexes (S1–S56). See DOI: **https://doi.org/10.1039/d3ob00229b**

tones, while simple mimics such as debranones require fewer steps and possess a high biological activity, comparable to that of the widely used strigolactone analogue GR24.[12,13] Other mimics, such as auxin-lactone, are synthesized in 3 steps and are more stable than GR24 under variable pH conditions. These mimics based on auxins are highly active against *P. ramosa* and exhibit a similar activity against *S. hermonthica* and *O. minor* when compared to strigolactones.[14] Lastly, there are stimulators of germination based on a phthalimide backbone, such as Nijmegen-1 and phthalimide-lactones (**PLs**), as the main representatives. Among the **PL** collection previously reported, some bioactivity profiles were similar to those of GR24 against *O. minor*, *P. aegyptiaca*, and *P. ramosa*. This is the case for **PL01**, **PL04**, **PL06**, **PL07**, or **PL14** (Figure Fig. 1), according to the results shown by Cala *et al.*[15] On the other hand, Nijmegen-1 has been tested in field trials, reducing the *S. hermonthica* population by ~65% in sorghum crops with a concentration of 1 μM.[16]

One of the major problems for the practical application of suicidal germination is the limited availability in soil. These compounds have poor water solubility due to their low polarity, which limits their application for large scale agrochemical purposes. There are different strategies to overcome this problem, but encapsulation is one of the most promising strategies with several advantages: no need to modify the bioactive structure, low-cost reagents and affordable simple synthesis methods, and a possibility for controlled release. We had success in previous studies with the synthesis of polymeric organic nanoparticles for the encapsulation of **PL01**, improving its water solubility more than twenty-five times.[7] However, a more direct and cheaper approach would be the use of cyclodextrins (**CDs**). Cyclodextrins are natural compounds with a cyclic structure of 6 (α-), 7 (β-), or 8 (γ-) units of α-D-glucose, and have a hydrophilic outer surface and a hydrophobic cavity. This cavity can be used to host organic molecules inside and obtain organic complexes with enhanced water solubility compared with the guest.[17,18] These complexes, like the β-cyclodextrin inuloxin complex, have been applied successfully in the past, and showed similar activity values to free inuloxin against *P. ramosa* without the addition of organic solvent.[19] We reported in a previous study the application of **CDs** with sesquiterpene lactones, which are germination inducers of *O. cumana* and *P. ramosa*. Water solubility and bioactivity were improved with this method.[20] In addition, **CDs** are authorized for human consumption by the European Food Safety Authority (EFSA) and the U.S. Food and Drug Administration (FDA)[21] and are considered environmentally friendly.

In this work, we have employed the natural **α-**, **β-**, and **γ-CD**, as well as 2-hydroxypropyl-β-cyclodextrin (**HP-β-CD**), which is one of the most used non-natural **CDs**, to study the host–guest complexes generated with three different phthalimide-lactones (**PL01**, **PL04**, and **PL07**). They have been chosen among the most active compounds against *P. ramosa* and other parasitic plants. Water solubility studies, bioactivity profiles, calorimetry analysis, complexation experiments, and semi-empirical *in silico* simulations have been carried out as part of the study to evaluate the potential of **CDs** for the encapsulation of strigolactone mimics.

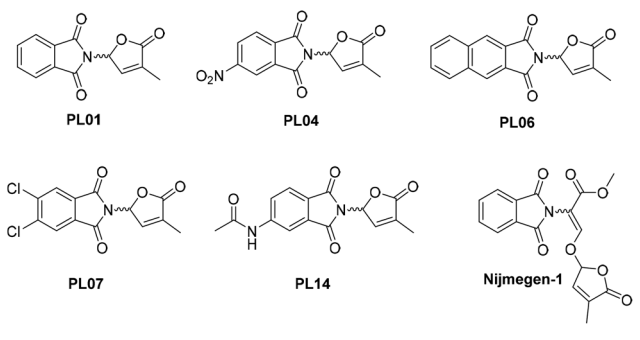

Fig. 1 Relevant structures of phthalimide-derived strigolactone mimics.

Results and discussion

Phase-solubility diagrams

Calibration curves for quantification were established by following a previously reported procedure,[20] using **PL01**, **PL04**, and **PL07** dissolved in MeOH as calibrators. Quantification was carried out by RP-HPLC with DAD (wavelength range 200–381 nm; see the Experimental section). Chromatograms exhibit two or more peaks (Fig. 2, top chromatograms), indicating a partial degradation of the compounds **PL01** and **PL04** in MeOH. The peak intensity of degradation products increased over time, so MeOH was discarded as a suitable solvent for the preparation of the standard solutions. Therefore, MeCN was selected as a solvent for standard solution preparation, due to its similar polarity to other organic solvents. In this case, the samples were stable for a very long time and only one peak was observed in the chromatograms even when the samples were injected days later (Fig. 2, bottom chromatograms), indicating suitable stability. However, the use of MeCN as sample solvent resulted in a slightly modified retention time as shown in the chromatograms in Fig. 2.

After calibration, the host–guest interaction of each compound with **α-**, **β-**, and **γ-CD** as well as **HP-β-CD** was studied using a modified Higuchi and Connors method that was reported recently.[20] The concentration of each phthalimide-lactone was measured for every experiment carried out with variations in the concentration of cyclodextrins by following the standard solubility diagram procedure. The **PL04** signal was not detected (LOD 0.025 mg mL^{-1}), neither in the cyclodextrin solutions nor in deionized water, indicating that the solubility was marginal even after interaction with cyclodextrins. Therefore, this compound was excluded from further studies. A reason for these results could be related to the different reactivities of **PL01** and **PL07**, when compared with **PL04**, which bears a nitro group at the aromatic ring. Polarity and charge distribution of the molecule are involved in the lack of supramolecular interaction of this phthalimide.[15]

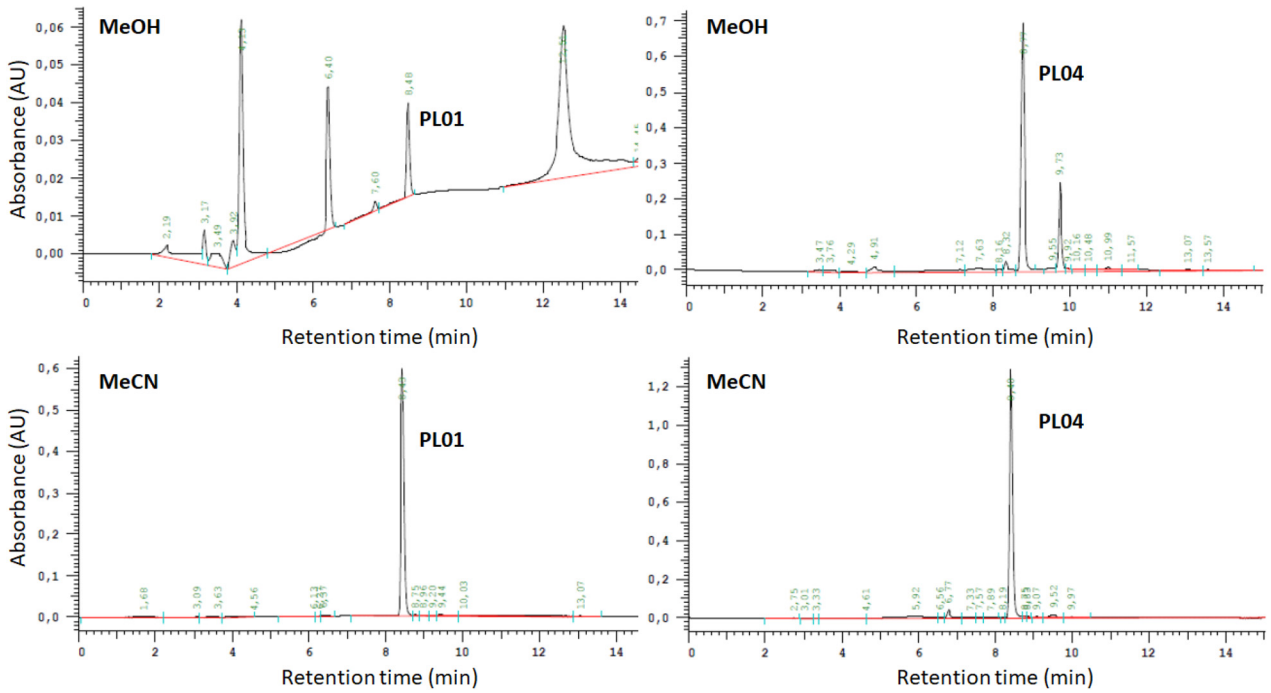

Fig. 2 Chromatograms obtained by RP-HPLC analysis (acquisition wavelength range: 200–381 nm) for samples dissolved in MeOH (**PL01** top left, **PL04** top right) and MeCN (**PL01** bottom left, **PL04** bottom right). Degradation peaks were observed in samples dissolved in MeOH. Retention time changes slightly when changing sample solvent.

Diagrams for α-CD with PL01 and PL07. Fig. 3 shows the phase solubility diagram for **PL01** and **PL07**. In the first case, **α-CD** barely interacted with any of the compounds. Concentrations of **PL01** changed almost imperceptibly with the increasing concentration of **α-CD**. The results obtained were fitted to a trendline, obtaining the following equation:

$$[\mathbf{PL01}] = 9 \times 10^{-4}[\mathbf{\alpha\text{-}CD}] + 0.111 \quad (1)$$

This adjustment produced $R^2 = 0.0413$, with a slope close to zero, indicating that no complex was formed. This could be associated with a B_S-type Higuchi–Connors diagram indicating that **CD** preferably forms self-assembled aggregates and the solubility of **CD** gradually increases even in the presence of the drug. An example of this behavior has been already reported by Schönbeck *et al.* in the formulation of hydrocortisone.[23] This is usually observed with really poorly-soluble drugs.

When using **PL07**, compound peaks were observed under only two conditions, both out of the calibration range (LOD 0.017 mg mL^{-1} and LOQ 0.052 mg mL^{-1}). These conditions were the values of 0 and 12 mM, and the estimated concentration values were very similar for both (2×10^{-3} and 3×10^{-3} mg mL^{-1}, respectively). No equation was reported in this case since only two unreliable data were obtained. Again, results did not hint at complex formation. In addition, this could also be explained by B-type diagrams.

Diagrams for β-CD with PL01 and PL07. In the case of **β-CD-PL01**, a linear trend was observed, indicating that the solubility increased linearly with a positive slope falling between 0 and 1 in the range of 0–10 mM **β-CD**, and these data were fitted to a trendline, obtaining $R^2 = 0.9542$ and the following equation:

$$[\mathbf{PL01}] = 2.44 \times 10^{-2}[\mathbf{\beta\text{-}CD}] + 0.113 \quad (2)$$

The final data of guest concentration at 12 mM were lower than the previous data at 10 mM, which may occur when the precipitation of a second less-soluble complex is produced at that concentration. The data fit to an A_L type diagram, indicating a 1 : 1 type complex in the straight slope. In these cases, as reported previously,[20] the complex constant ($K_{1:1}$) and the complexation efficiency (CE) were determined using the following equations:

$$K_{1:1} = \frac{\text{Slope}}{S_0 \cdot (1 - \text{Slope})} \quad (3)$$

$$\text{CE} = S_0 \cdot K_{1:1} = \frac{\text{Slope}}{1 - \text{Slope}} \quad (4)$$

where S_0 is the solubility of each **PL** in H_2O at 0 mM [**CD**]. In this case, by applying eqn (3) and (4), S_0 = 0.104 mM, $K_{1:1}$ = 240 M^{-1} and CE = 0.025. The complexation constant is similar to that obtained for (−)-α-santonin with previously reported **β-CD**,[20] although the CE indicates a low efficiency in the complexation process, thus predicting a low increase of solubility of the solid complex when compared with the free **PL01** in water.

Regarding **PL07**, the concentrations detected were not much higher than in the case of **α-CD**, and still out of the calibration range. This could be explained by the higher molecular

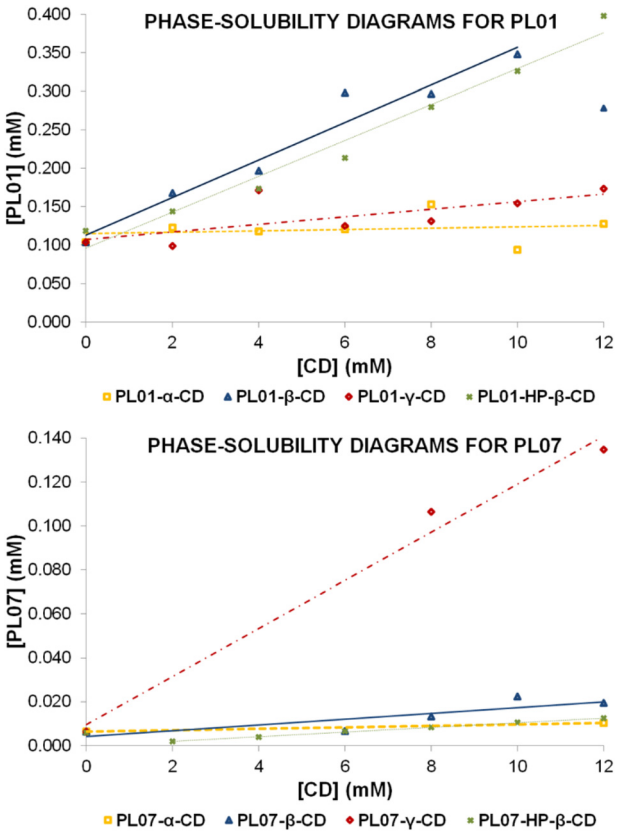

Fig. 3 Phase-solubility diagrams obtained by following the Higuchi and Connors method[20,22] for **PL01** (top) and **PL07** (bottom) with 4 different cyclodextrins: **α-** (orange), **β-** (blue), **γ-** (red), and **HP-β-CD** (green). Concentration of each sample was measured after treatment with **CD** in a range of 0–12 mM.

volume exhibited because of two chlorine atoms that are substituted in the aromatic ring. Data are fitted using the following equation:

$$[\mathbf{PL07}] = 1.30 \times 10^{-3}[\boldsymbol{\beta}\textbf{-CD}] + 0.004 \quad (5)$$

Fig. 3 seems to show a linearly increasing tendency. However, the slope was very low and the goodness of the adjustment value was only R^2 = 0.7033. It can be considered that the interactions of **PL07** with **β-CD** are stronger than those with **α-CD**, but still weak. The observed data suggest the formation of a 1 : 1 complex, although the results were not satisfactory enough for a confident calculation of $K_{1:1}$ and CE.

Diagrams for γ-CD with PL01 and PL07. The phase solubility diagram for **PL01** with **γ-CD** indicated again a linear increase of solubility with the concentration of **CD**, with a positive slope falling between 0 and 1 and R^2 = 0.9184, obtaining the following equation:

$$[\mathbf{PL01}] = 5.90 \times 10^{-3}[\boldsymbol{\gamma}\textbf{-CD}] + 0.093 \quad (6)$$

The slope in this case is higher than that in the experiment with **α-CD**, implicating stronger interactions with **γ-CD**. However, the slope is still low when compared with the value for **β-CD**. By applying eqn (3) and (4), S_0 = 0.104 mM, $K_{1:1}$ = 57 M^{-1} and CE = 0.006, which, as expected by observing the shape of the diagram, indicates a lower efficiency of the complexation process, which will cause a small increment in the solubility of the complex when compared with free **PL01**.

As in the previous two cases, complexation with **PL07** worked worse than that with **PL01** when using **γ-CD**, and also the measurements were out of the calibration range, obtaining only three valid measurements. Nevertheless, in this experiment, when using 8 and 12 mM **γ-CD**, the concentration of **PL07** increased in a higher degree, as observed in the areas of the peaks. As in the case with **β-CD**, a trendline was obtained to get conclusions:

$$[\mathbf{PL07}] = 1.09 \times 10^{-2}[\boldsymbol{\gamma}\textbf{-CD}] + 0.096 \quad (7)$$

This equation has R^2 = 0.985, indicating a linear increase of the solubility, still very low, but with a higher slope than in the previous cases, suggesting stronger interactions of **PL07** with this **CD**. By observing the data, a 1 : 1 complex could be hypothesized, although the results were not satisfactory enough for a confident calculation of $K_{1:1}$ and CE.

Diagrams for HP-β-CD with PL01 and PL07. The solubility diagram developed with **HP-β-CD** and **PL01** presents a different tendency, away from a linear diagram A_L (Fig. 4a). In this case, a positive deviation from linearity (A_P type) can be observed, suggesting the formation of a higher-order complex with respect to **CD**.[24] According to the data, two cyclodextrins host one molecule of **PL01**.

$$\mathbf{HP-\beta-CD} + \mathbf{PL01} \overset{K_{1:1}}{\rightleftharpoons} \mathbf{HP-\beta-CD \cdot PL01}$$

$$\mathbf{PL01 \cdot HP-\beta-CD} + \mathbf{HP-\beta-CD} \overset{K_{1:2}}{\rightleftharpoons} \mathbf{PL01 \cdot 2HP-\beta-CD}$$

The system settled out in equations allows us to get the binding constants of Higuchi–Connors diagrams by:

$$\frac{[\mathbf{PL01}]_t - [\mathbf{PL01}]_0}{[\mathbf{HP-\beta-CD}]_t} = K_{1:1} \cdot [\mathbf{PL01}]_0 + K_{1:1} \cdot K_{1:2} \cdot [\mathbf{PL01}]_0 \cdot [\mathbf{HP-\beta-CD}]_t \quad (8)$$

Table 1 shows binding constant values calculated from experimental data. This result differs from those of other PL solubility studies. Different assays carried out with **α-**, **β-**, and **γ-CD** showed 1 : 1 type complexation. In addition to that, no other **PLs** presented a different complex but the 1 : 1 host–guest. Comparing inner cavity sizes, **γ-CD** presents a portal diameter between 7.5 and 8.3 Å, while **HP-β-CD** presents values between 6.0 and 6.4 Å.[25] Simplicity of **PL01**, without voluminous functional groups in the main structure, does not help to understand the formation of the postulated 1 : 2 complex. Due to that, isothermal titration calorimetry (ITC) was developed to confirm the results (Fig. 4c and d).

The performed ITC experiment confirmed the Higuchi–Connors results. Fig. 4d shows that the stoichiometry of the system is N = 2. Furthermore, Table 1 shows that K_{obs} values calculated with both approaches are quite similar.

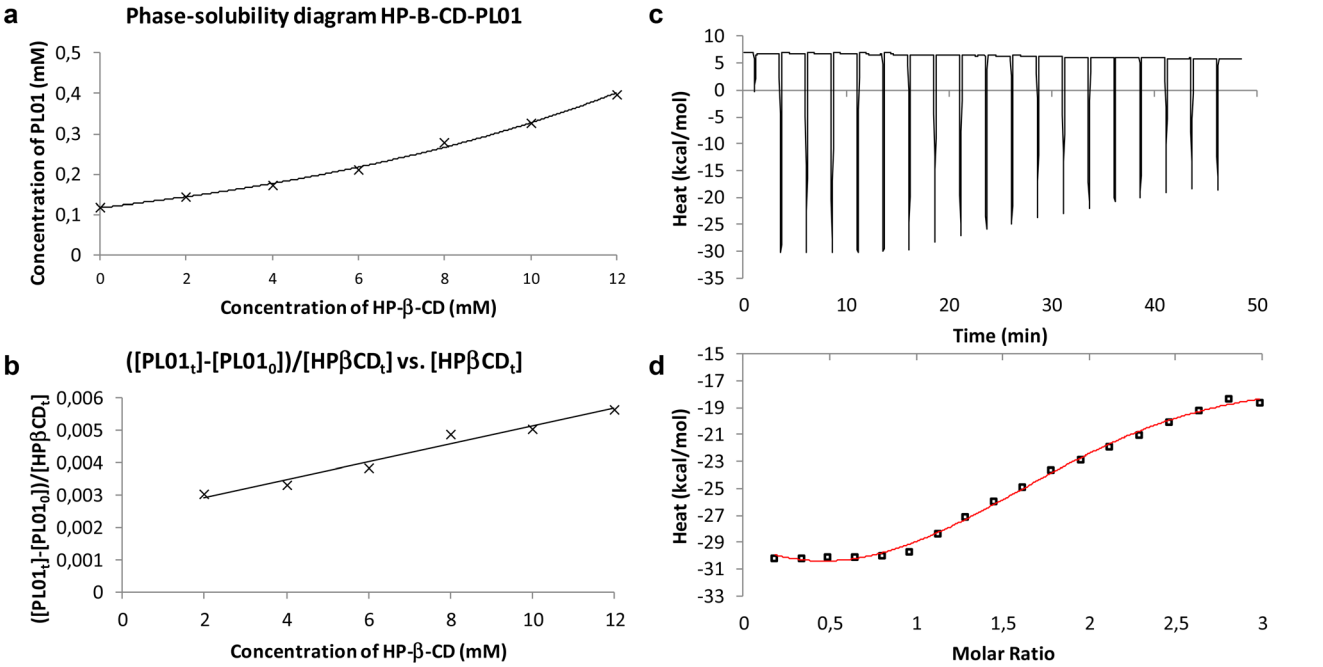

Fig. 4 (a) Higuchi–Connors solubility diagram between **HP-β-CD** and **PL01**. (b) Representation of the **PL01/HP-β-CD** ratio to calculate binding constants. (c) Titration calorimetry diagram between **HP-β-CD** (8.00×10^{-4} M) and **PL01** (5.00×10^{-5} M) in deionized water. (d) Representation of thermodynamic values obtained from titration calorimetry studies.

Table 1 Comparison of Higuchi–Connors *vs.* ITC binding constants

Method	$K_{1:1}$, $K_{1:2}$ (M^{-1})	K_{obs} (M^{-1})
Higuchi–Connors	8.276×10^{-4}, 1.250×10^{-4}	10.34×10^{-5}
ITC	—	$(6.63 \pm 1.88) \times 10^{-5}$

Experimental enthalpy obtained from Fig. 4d is $\Delta H = -323.0 \pm 48.7$ kcal mol^{-1} and $-T\Delta S = 318.0$ kcal mol^{-1}, so 1 : 2 host–guest complexation is spontaneous with $\Delta G = -5.71$ kcal mol^{-1}. From Fig. 4a, it can be observed that the water solubility of **PL01** when **HP-β-CD** was applied was enhanced around 3 times. Taking into account the results of the performed experiments, it is suggested that the small structure of **PL01** makes the approach of a new cyclodextrin molecule to establish intermolecular forces among branched functional groups (2-hydroxypropyls) possible, generating a capsule-like complex of **PL01**. This differs from **PL07** because its functional groups already would have established interactions with hydroxypropyl groups, without the possibility of a further cyclodextrin coordination. In fact, the interactions of **PL07** were still weaker than those with the other **CDs**, indicating that there is not a huge difference with the inclusion of the hydroxypropyl groups. In this case, the increase of solubility was similar to that of the **β-CD** diagram (with a similar slope), following a linear trend with the increase of **CD** concentration. However, the values were out of the calibration range and the concentration of **PL07** decreased at lower concentrations of **CD** to increase later to a higher concentration than that at 0 mM. This indicates two linear trends. An adjustment of the data in the second trend (starting at 2 mM) produced the following equation:

$$[\mathbf{PL07}] = 1.1 \times 10^{-3}[\mathbf{HP\text{-}\beta\text{-}CD}] + 0.001 \quad (9)$$

with a very good value of $R^2 = 0.9989$, demonstrating clearly the difference between **PL01** and **PL07** interactions with this **CD**, and suggesting a 1 : 1 complex, although the results were not satisfactory enough for a confident calculation of $K_{1:1}$ and CE.

Preparation of the solid complexes

The complexes were prepared by following the co-precipitation method according to our previous findings,[20] where precipitation of the corresponding complexes (as a white precipitate) was observed shortly after adding the dissolved guests into the solution of cyclodextrin for the cases of **PL01** and **PL07** with **β-**, **γ-**, and **HP-β-CD**. The amount of the observed precipitate increased significantly as the complexation reaction was approaching the end. This is expected, since the **CD**-complexes are expected to be less soluble in water than the free **CDs**, and the concentrations were adjusted to be close to the solubility limits of free **CDs**. After that, the solutions were concentrated and dried to recover as much precipitate as possible. However, a low amount of precipitate was obtained for **α-CD**, which was expected, since almost negligible interaction was observed in the phase-solubility diagrams. Nevertheless, the reaction was treated in the same way, in order to obtain as much complex as possible and analyze the sample in the bioassays and the solubility measurements. Compound **PL04** was not employed,

since the phase-solubility diagram did not show evidence of interaction with the **CDs** employed and the peaks for this compound were not found in the chromatograms. Stoichiometry was employed as the phase-solubility diagram suggested, and therefore 1 : 1 was considered for all the cases, except for **PL01** and **HP-β-CD** where 1 : 2 was employed instead. The employed concentration of **β-CD** was lower than the rest of the cases since it is the least water soluble among all the **CDs** employed, although, the relative molar amounts of the guest and host were adjusted to maintain the expected stoichiometry (see the Experimental section).

Solubility studies

The aliquots of saturated solutions of each **CD** complex and free **PL** were injected into the RP-HPLC system by following the method reported in the Experimental section and the areas of the peaks were used to calculate the concentration of each original sample. Solubility ratios were calculated using eqn (10), to compare the efficiency of the different cyclodextrins to increase the solubility of the compounds (Table 2).

$$\text{Solubility ratio} = \frac{[\text{Compound in the complex}]}{[\text{Free compound}]} \qquad (10)$$

At a first glance of the results, it was appreciated that they were in agreement with the phase-solubility diagrams: weak interactions with the **CDs** translated into low increments of the solubility in water. By comparison of the different solubility ratios, the best results when comparing the different natural **CDs** were obtained with **β-CD** for both compounds, with an increase of solubility of almost 3 times the original in the case of **PL01**, and a discrete increase in the case of **PL07**. Though this **CD** is the least soluble among the three, its interactions and cavity size may have played a significant role.[26] When comparing both **β-CD** and **HP-β-CD**, the increases of solubility are even higher for **PL01**, with almost quadruple of the initial solubility in water, and in the case of **PL07**, this increase doubles. These findings indicate that even when a weaker interaction with **CDs** is produced (the case of **PL07**), the selection of a more soluble **CD** with an appropriate cavity size may help to obtain a higher solubility. On the other hand, although the solubility increases obtained for **α-CD** are comparable to those of **γ-CD**, the lack of interactions suggested by the solubility diagrams may imply that these solubility increases are caused by an adjuvant or micellar effect rather than proper complexation.[27,28]

Molecular modelling

Semiempirical optimizations (PM3 calculation level) were carried out to compare the results of the experiments with the processes happening at a molecular level. They were carried out using Hyperchem® and more details about the conditions can be found in the Experimental section.

In the first case, it was observed that both **PL01** and **PL07** did not fit inside the **α-CD** cavity, thus explaining the weak interactions with this **CD**. The geometry optimization was then carried out with **β-**, **γ-**, and **HP-β-CD**, with bigger cavity sizes. The calculated energies of the geometry optimizations are shown in Table 3, while Fig. 5 shows the images of the most stable complexes shaded in gray in the table. The images of the least stable complexes and the separated model are shown in the ESI (S1–S56†).

The most stable models were **PL01-β-CD (C)**, **PL01-γ-CD (E)**, **PL01-HP-β-CD (D)**, **PL01-HP-β-CD (B4)**, **PL07-β-CD (A)**, **PL07-γ-CD (A)**, and **PL07-HP-β-CD (D)**. In all the cases, **PL01** and **PL07** fitted at least partially inside the cavity of the **CDs**, although **PL01** was hosted completely in the case of **PL01·γ-CD (E)**.

Regarding **PL01**, the furanone ring inside the cavity was the most stable geometry in the case of **β-CD** (**PL01-β-CD (C)**), while for **γ-CD** (**PL01-γ-CD (E)**), the molecule was fully hosted (Fig. 5). None of the complexes of **PL01-β-CD** were more stable than the separate model as indicated for $\Delta E_{PM3} > 0$, which is the opposite case for **PL01-γ-CD**, therefore indicating a higher stabilization of the structure when surrounded by the **CD**, which can be observed again in the models with **HP-β-CD** (**PL01-HP-β-CD (D)** and **PL01-HP-β-CD (B4)**). The highest stabilization was obtained for the **HP-β-CD** complexes, where the energy stabilization was higher (in absolute terms) for the 1 : 1 model (−361.78 kJ mol^{-1}) than the 1 : 2 model (−292.80 kJ mol^{-1}). However, these values are in the same order of magnitude and this discrepancy is caused by the change in con-

Table 2 Solubility ratios of cyclodextrin (**CD**) complexes

Compound	mg mL^{-1}	mM	Solub. (0 mM **CD**)	Solub. ratio ± SD
PL01-α-CD	0.060	0.247	0.104	2.41 ± 0.06
PL01-β-CD	0.073	0.300		2.86 ± 0.04
PL01-γ-CD	0.055	0.225		2.25 ± 0.15
PL01-HP-β-CD	0.097	0.398		3.82 ± 0.01

Compound	Mean area[a] (complex)	Mean area[a] (0 mM **CD**)	Solub. ratio[b] ± SD
PL07-α-CD	12 869	14 128	0.91 ± 0.62
PL07-β-CD	16 848		1.26 ± 0.12
PL07-γ-CD	14 560.5		1.03 ± 0.12
PL07-HP-β-CD	27 496		1.95 ± 0.01

[a] For those with values out of the calibration range, mean areas of the peaks instead of concentrations were employed. [b] Increase of solubility was obtained from mean area quotient.

Table 3 Complexation stabilization energy values (kJ mol^{-1}) after geometry optimization of the complexes and the separate molecules with the PM3 calculation level including 250 (**PL01·β-CD**, **PL01·γ-CD**, **PL01·HP-β-CD** **PL07-β-CD**, and **PL07-γ-CD**) or 222 (**PL01-HP-β-CD** (1 : 2) and **PL07-HP-β-CD** (1 : 1)) molecules of H_2O. Four different orientations of the **PLs** were used, except for **PL01-HP-β-CD** (Fig. 5 and ESI S1–S56†), the most stable is shaded in gray. The complexation stabilization values for ΔE_{PM3} were calculated as $E_{complex} - E_{separate}$

Complex	E_{PM3} (kJ mol^{-1})	ΔE_{PM3} (kJ mol^{-1})	Complex	E_{PM3} (kJ mol^{-1})	ΔE_{PM3} (kJ mol^{-1})
Separate PL01 and β-CD	−304 260.90	—	**Separate PL07 and β-CD**	−304 035.17	—
PL01-β-CD (A)	−304 022.01	238.89	**PL07-β-CD (A)**	−303 989.81	45.35
PL01-β-CD (B)	−304 009.19	251.71	**PL07-β-CD (B)**	−303 866.00	169.16
PL01-β-CD (C)	−304 147.37	113.53	**PL07-β-CD (C)**	−303 751.73	283.43
PL01-β-CD (D)	−304 044.06	216.83	**PL07-β-CD (D)**	−303 774.74	260.43
Separate PL01 and γ-CD	−312 689.03	—	**Separate PL07 and γ-CD**	−312 614.77	—
PL01-γ-CD (A)	−312 641.74	47.29	**PL07-γ-CD (A)**	−312 620.80	−6.03
PL01-γ-CD (B)	−312 580.88	108.14	**PL07-γ-CD (B)**	−312 512.25	102.52
PL01-γ-CD (C)	−312 455.16	233.87	**PL07-γ-CD (C)**	−312 336.61	278.17
PL01-γ-CD (D)	−312 500.68	188.34	**PL07-γ-CD (D)**	−312 336.79	277.98
PL01-γ-CD (E)	−312 747.26	−58.24	**PL07-γ-CD (E)**	−312 539.93	74.85
Separate PL01 and HP-β-CD	−334 304.35	—	**Separate PL07 and HP-β-CD**	−334 030.39	—
PL01-HP-β-CD (A)	−334 232.04	−201.66	**PL07-HP-β-CD (A)**	−334 127.13	−96.74
PL01-HP-β-CD (B)	−334 235.39	−205.01	**PL07-HP-β-CD (B)**	−334 091.23	−60.84
PL01-HP-β-CD (C)	−334 162.83	−132.45	**PL07-HP-β-CD (C)**	−334 229.54	−199.16
PL01-HP-β-CD (D)	−334 392.16	−361.78	**PL07-HP-β-CD (D)**	−334 297.84	−267.45
Separate PL01 and HP-β-CD	−395 306.97	—			
PL01-HP-β-CD (A1)	−395 252.57	54.40	**PL01-HP-β-CD (C1)**	−395 001.03	305.95
PL01-HP-β-CD (A2)	−395 386.26	−79.28	**PL01-HP-β-CD (C2)**	−395 135.77	171.20
PL01-HP-β-CD (A3)	−395 328.48	−21.51	**PL01-HP-β-CD (C3)**	−395 214.73	92.24
PL01-HP-β-CD (A4)	−395 342.55	−35.57	**PL01-HP-β-CD (C4)**	−395 115.85	191.13
PL01-HP-β-CD (A5)	−395 244.44	62.53	**PL01-HP-β-CD (C5)**	−395 114.58	192.39
PL01-HP-β-CD (A6)	−395 239.05	67.93	**PL01-HP-β-CD (C6)**	−395 179.94	127.03
PL01-HP-β-CD (B1)	−395 392.53	−85.56	**PL01-HP-β-CD (D1)**	−395 190.16	116.81
PL01-HP-β-CD (B2)	−395 376.07	−69.10	**PL01-HP-β-CD (D2)**	−395 238.79	68.18
PL01-HP-β-CD (B3)	−395 553.86	−246.89	**PL01-HP-β-CD (D3)**	−395 326.65	−19.68
PL01-HP-β-CD (B4)	−395 599.77	−292.80	**PL01-HP-β-CD (D4)**	−395 203.05	103.92
PL01-HP-β-CD (B5)	−395 394.30	−87.33	**PL01-HP-β-CD (D5)**	−395 090.49	216.49
PL01-HP-β-CD (B6)	−395 400.09	−93.12	**PL01-HP-β-CD (D6)**	−395 117.69	189.28

ditions, since more water molecules were employed in this model than in the 1 : 2 models due to the limitations of software. It is expected that by including a higher number of water molecules the energy values will become lower for the 1 : 2 complex. In addition, it has been stated before[29] that complexation with **CDs** is an equilibrium where more than one species can co-exist in solution, suggesting the co-existence of both complexes in solution. The highest stabilization for **HP-β-CD** when compared with the other two **CDs** explains the higher increases in the solubility of the obtained complexes, the higher slopes and the better bioactivity results.

On the other hand, results for stabilization energy for the models of **PL07** were very discrete for **β-CD** (**PL07-β-CD (A)** = 45.35 kJ mol^{-1}) and **γ-CD** (**PL07-γ-CD (A)** = −6.03 kJ mol^{-1}), which were positive and slightly negative, respectively. This correlates with the small solubility ratios for this compound, which were only improved by **HP-β-CD**, which presents the highest stability for this compound (**PL07-HP-β-CD (D)** = −267.45 kJ mol^{-1}).

In this case, the geometry of this model shows that **PL07** is completely surrounded by the **CD** and the furanone ring interacts with the isopropyl residues. This interaction could be crucial for the increase in stability since the slightly more soluble **γ-CD** complex presents a model where this ring is close to the –CH_2OH fragments (hydrophilic outer ring), while in the **β-CD** model, the phthalimide ring was located in this part. The weaker interaction of the **CDs** with **PL07** than with **PL01** also explains the slightly lower bioactivity of **PL07**-complexes *vs.* free-**PL07**.

Bioassays on parasitic weeds

The induction of germination of *P. ramosa* seeds was tested for the **PLs**, **CDs** and their complexes by following the procedure already described in the literature.[30] The free compounds **PL01** and **PL07** were predissolved in acetone (1% v/v) and then diluted with water. On the other hand, the complexes were directly dissolved in water without a co-solvent. In all the cases, complexes with natural **CDs** (α-, β-, and γ-) showed similar levels of bioactivity in comparison with the bioactivity of the **PLs** without **CDs**, even without the use of an organic co-solvent (Fig. 6A). An increase of bioactivity was observed at the third dilution (1 μM) when comparing **PL01-α-CD** and **PL01-β-CD** with **PL01**, while a decrease was observed for **PL01-γ-CD**. On the other hand, the bioactivity decreased at the fourth dilution (0.1 μM) for all the **PL01** complexes. Regarding **PL07**, it was observed that the bioactivity profile was slightly impaired

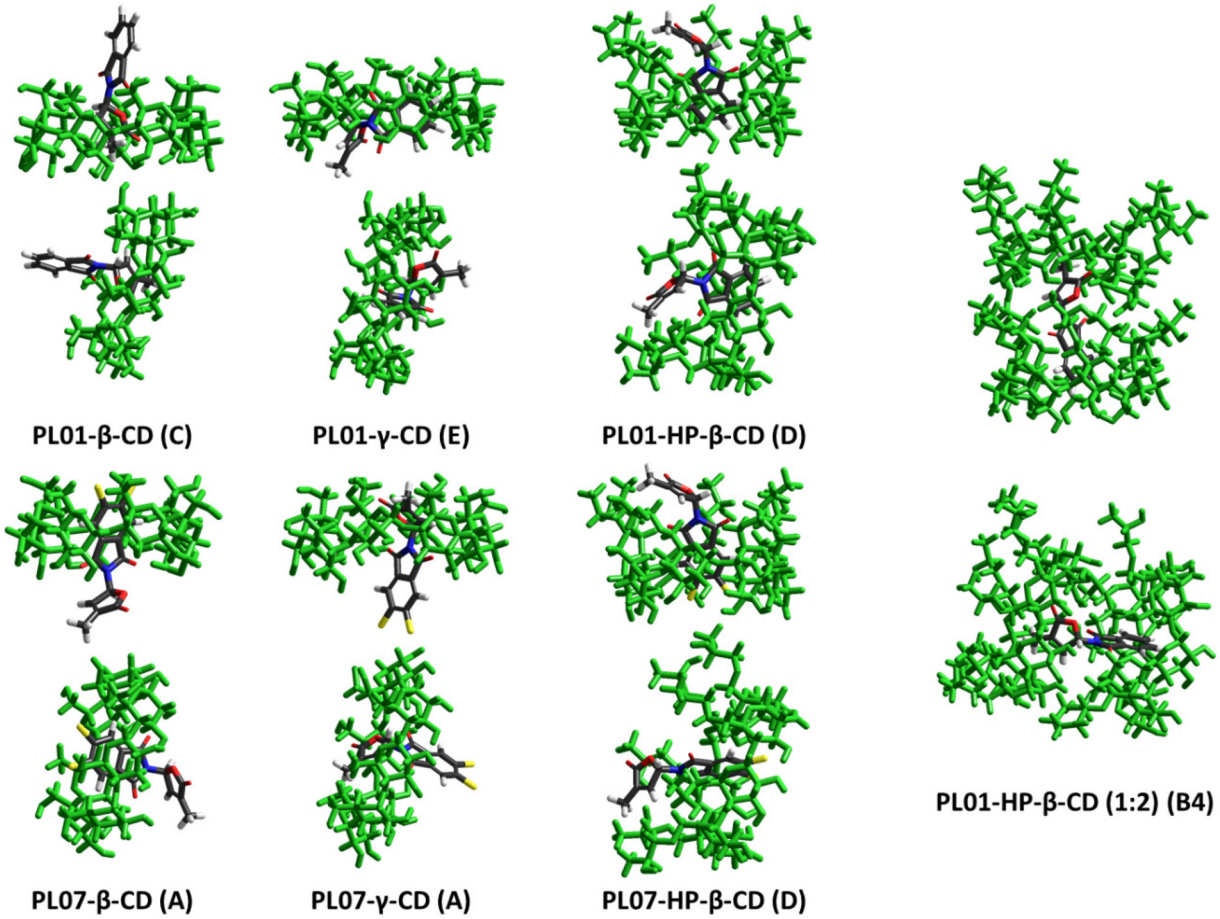

Fig. 5 Images of the geometrically optimized theoretical complexes of **PL01** and **PL07** with **β-**, **γ-**, and **HP-β-CD** with the most stable orientations of the complexes. H_2O molecules are hidden for the sake of clarity. Least stable optimizations, as well as high quality images for the stable complexes, are available in the ESI (S1–S56†).

for the complexes, starting at the third dilution and, especially, at the fourth dilution, the bioactivity dropped dramatically. This is correlated with theoretical simulations, which exhibited weak interactions of **PL07** with the three **CDs** and therefore a lower increase of solubility of the complex. Nevertheless, these results imply that these compounds can be applied in a formulation for the fight against parasitic plants without organic solvents. In the case of **HP-β-CD** (Fig. 6B), the bioactivity was, in general, increased when compared with the free **PLs** even at the lowest concentration. The bioactivity of **PL01-HP-β-CD** was increased for the complex in correlation with the phase-solubility diagrams, where strong host–guest interactions were observed. The complex **PL07-HP-β-CD** showed high water solubility, and its bioactivity was slightly better than **PL07-β-CD**, although both complexes present similar interaction energy. It is likely that cyclodextrins exert an influence on bioavailability and not only on the water solubility.

Activity on *O. cumana* was also tested, finding only activity at the highest concentration tested (100 μM), although the effect of treatment with cyclodextrins on the bioactivity was similar (similar or slight increase of germination). Compounds tested did not induce germination of *O. crenata* and the positive control **GR24** only induced moderate germination. A deviation in the bioactivity results compared with previous studies[7,15] is expected for this bioassay because of the season, age of the seeds and other environmental factors.[31] In general, it was observed that encapsulation with cyclodextrins not only preserved the bioactivity of the pure compounds but also increased it in some cases. This bioactivity was also observed using completely aqueous test solutions.

Avoiding the use of organic co-solvents, such as acetone or DMSO that are common in this kind of bioassays, by formulation with cyclodextrins is not only a greener choice, but also decreases the possibilities of precipitate formation by the evaporation of the prior, improving the potential for practical use in preparations as future commercial herbicides.

Experimental

General experimental procedures

Complexation reactions were carried out on a Heidolph Synthesis 1 at a controlled temperature and constant stirring. RP-HPLC analysis was carried out using a VWR Hitachi

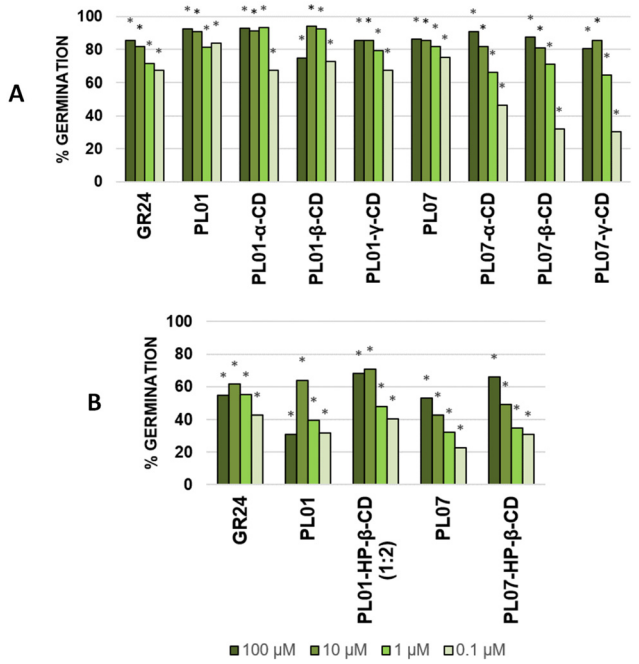

Fig. 6 Activity on the germination of *P. ramosa* seeds. Germination (%) was calculated by comparison with the germination rate of negative control (water). Significance of the data is indicated with an asterisk (*) over each significant value assessed by Dunnett's test (p 0.05). Each assay was performed with a different batch of seeds; (A) results for **α-**, **β-** and, **γ-CD** and (B) results for **HP-β-CD**.

Chromaster equipped with a DAD model 5430 and a Phenomenex Gemini C_{18} 250 × 4.6 mm column with a 5 μm particle diameter and 110 Å pore size in gradient mode. HPLC gradient quality solvents were supplied by Avantor (Pennsylvania, USA). Sigma-Aldrich Co. (St Louis, Missouri), Merck (Darmstadt, Germany), Alfa Aesar (Ward Hill, Massachusetts) or TCI (Oxford, UK) supplied the reagents. Parasitic weed seeds were kindly provided by professors Leonardo Velasco (CSIC, Córdoba, Spain) and Maurizio Vurro (National Research Council – Institute of Sciences of Food Production, Bari, Italy).

Synthesis of phthalimide-lactones

PL01, **PL04**, and **PL07** were synthesized using the procedure described in the literature.[15]

Calibration of phthalimide-lactones in RP-HPLC

Eight standard solutions of each compound **PL01**, **PL04**, and **PL07** (0.025–1 mg mL^{-1}) were used to calibrate the RP-HPLC system. The method consisted a 15 min gradient at room temperature starting at 7 : 3 H_2O : MeCN (see Table 4), a flow of 1 mL min^{-1}, a re-equilibration time of 4 min and a 10 μL injection volume. Due to the low solubility of PLs in H_2O, samples were dissolved in MeCN (or at the beginning in MeOH) and filtered through a 0.45 μm nylon syringe filter (25 mm, Scharlau NYL2545200) prior to injection. The chromatograms were acquired in triplicate using a DAD set in the wavelength range of 200–381 nm, using the integrated chromatogram setting to measure the areas bellow the peaks. Retention times for each compound were 8.18 (±0.10), 8.33 (±0.07) and 9.71 (±0.03) minutes for **PL01**, **PL04** and **PL07**, respectively.

Table 4 Conditions for the PL analysis method by RP-HPLC at a flow of 1 mg mL^{-1}

Time (min)	0	5	7	9	11	13	15
% MeCN	30	70	70	100	100	30	30

The correlations between the mean areas of the peaks in the chromatograms and the concentrations of each phthalimide-lactone were stablished using two ranges, the first one including the lower concentrations (0.025–0.250 mg mL^{-1}) and the second for the higher concentrations (0.250–1.000 mg mL^{-1}). In both ranges, the coefficients were R^2 = 0.9991 (**PL01**), 0.9946 (**PL04**), and 0.9973 (**PL07**) for the lower range; and R^2 = 0.9802 (**PL01**), 0.9799 (**PL04**), and 0.9767 (**PL07**) for the higher range. The correlations were considered good enough to be used in the next experiments, by employing the resulting eqn (1)–(6). LOD and LOQ were as follows: 0.010 mg mL^{-1} and 0.030 mg mL^{-1} (**PL01**), 0.025 mg mL^{-1} and 0.075 mg mL^{-1} (**PL04**), and 0.017 mg mL^{-1} and 0.052 mg mL^{-1} (**PL07**).

$$C(\mathbf{PL01}) = \frac{\text{Area} - 41\,709}{6 \times 10^6}\ \text{mM} \quad (11)$$

$$C(\mathbf{PL01}) = \frac{\text{Area} - 1\,000\,000}{2 \times 10^6}\ \text{mM} \quad (12)$$

$$C(\mathbf{PL04}) = \frac{\text{Area} - 33\,917}{7 \times 10^6}\ \text{mM} \quad (13)$$

$$C(\mathbf{PL04}) = \frac{\text{Area} - 930\,509}{4 \times 10^6}\ \text{mM} \quad (14)$$

$$C(\mathbf{PL07}) = \frac{\text{Area} - 57\,742}{7 \times 10^6}\ \text{mM} \quad (15)$$

$$C(\mathbf{PL07}) = \frac{\text{Area} - 1\,000\,000}{3 \times 10^6}\ \text{mM} \quad (16)$$

Phase-solubility diagrams for the complexation of phthalimide-lactones by HPLC

Solubility studies were carried out by following a modified Higuchi and Connors method[22] which was reported previously.[20] An excess of **PL01**, **PL04**, or **PL07**, above their solubility in H_2O (2–3 mg) was added to aliquots of 5 mL of each **CD** in a concentration range of 0–12 mM in each tube. The concentrations of the compounds in these aliquots were evaluated by RP-HPLC using the methods and the equations described previously for calibration curve establishment. As previously reported for sesquiterpene lactones,[20] the retention times for the peaks of phthalimide-lactones changed slightly in comparison with the standard depending on the **CD** concentration (by less than one minute).

ITC

Isothermal titration calorimetry was employed to confirm the 1 : 2 complex formation between **PL01** and **HP-β-CD** deduced

from the phase-solubility diagrams. MicroCal PEAQ-ITC was kindly supplied by Malvern® to carry out the experiment. **PL01** was placed in the cell of the ITC with a concentration of 5.00×10^{-5} M and 2-hydroxypropyl-β-cyclodextrin was continuously added (8.00×10^{-4} M) during 20 injections at 25.3 °C (2.00 μL per injection). The experiment was performed in Milli-Q water and stirred at 750 rpm.

Preparation of the solid complexes

Based on our previous findings with sesquiterpene lactones,[20] the co-precipitation method was chosen and the following conditions were used: 5.4 mg of **PL01** (0.022 mmol) or 6.9 mg **PL07** (0.022 mmol) were dissolved in 500 μL MeCN and added dropwise to 1.25 mL of a **β-CD** solution (17.6 mM) in deionized H_2O. The same amount of either **PL01** or **PL07** was dissolved in 200 μL or 400 μL MeCN and added dropwise to 500 μL of **α-CD** (44 mM) or **γ-CD** (44 mM) aqueous solutions to prepare the corresponding complexes of **α-** and **γ-CD**, respectively. In the case of **HP-β-CD**, 0.022 mmol of **PL01** were dissolved in 200 μL MeCN and added dropwise to 500 μL of **HP-β-CD** (88 mM) and 0.025 mmol of **PL07** were dissolved in 446 μL MeCN and added dropwise to 500 μL of **HP-β-CD** (49 mM). Additions were carried out while stirring at room temperature for 72 h, then the solvents were removed on a rotatory evaporator at 50 °C and dried overnight in a vacuum at 37 °C to remove any remaining H_2O.

Solubility measurements

Each complex and each phthalimide-lactone evaluated (**PL01**, **PL04**, and **PL07**) were separately added in excess to tubes containing 5 mL deionized H_2O and stirred at 25 °C until no more solid dissolved. Each tube was centrifuged at 4400 rpm, the supernatant filtered through a 0.45 μm nylon syringe filter and an aliquot of 1 mL was analyzed by RP-HPLC. In order to minimize the measurement error, samples of complexes were analyzed in triplicate and samples of phthalimide-lactones in quintuplicate. Concentration was obtained using the calibration equations reported above to calculate the solubility of each compound.

Molecular modelling

Computational studies were carried out by using the software HyperChem v7.5 for Windows (Hypercube, Inc.) to predict the most stable geometries of the hypothetical complexes in H_2O. Periodic boxes were built by including the guest (**PL01** or **PL07**), the host (**β-**, **γ-**, or **HP-β-CD**) and a solvation shell of H_2O molecules. Compound **PL04** was not included among the calculations since no interaction was found in the phase-solubility diagrams. Since the interaction with **α-CD** was almost negligible and assumed to be related to a micellar effect rather than a complexation phenomenon, this **CD** was also excluded. Two kinds of aggregates were designed: separate host and guest, and guest inserted into the host. The size of the periodic boxes was initially set to fit 250 molecules of H_2O as reported previously;[20] however, the high use of RAM memory (over 1 GB) when optimizing the geometry of the complexes with **HP-β-CD** caused an error of exhausted memory after the 10th iteration (first cycle) due to limitations of the software. In order to avoid this problem, the periodic box sizes for this **CD** were adjusted to contain a total of 222 H_2O molecules (in random positions in the box), which were manageable for the software in all the cases without errors. The model for **HP-β-CD** was based on PDB 3CGT and built as reported previously,[32] the models for the other **CDs** were already reported,[20] and the **PLs** were built on ChemDraw v20.1 (PerkinElmer) and their geometry was pre-optimized in a vacuum using PM3, which is the same level of calculation for the host–guest-solvation water complex. Since the employed **PLs** possess a stereochemical center, the same enantiomer, with *S*-stereochemistry (***S*-PL01** and ***S*-PL07**), was built in the three cases (**β-**, **γ-**, or **HP-β-CD**) to allow comparison. Geometry optimizations for the supramolecular systems were carried out using PM3. Four possible insertions (A–D) of the guests into the hosts and a last additional calculation with separate guests and hosts were considered for the 1 : 1 complexes with **β-CD**, considering that the **PL** could approach, either through the lactone or the phthalimide backbone, the hydrophilic or lipophilic part of the **CD**. A fifth possible insertion was also considered in the bigger **γ-CD (E)** where the molecules fit inside the cavity in the horizontal position. Since the complex of **PL01** with **HP-β-CD** was found to be a 1 : 2 type complex, this was also taken into consideration and the system was built accordingly, increasing the amount of possible insertions to 24 by combining the different orientations of **PL01** with the possibilities of the **PL** approaching both **CDs** in a 90° position adding to the original insertions already considered in the other **CDs** (for a total of 6 possibilities, models with numbers 1–6) and 4 possible orientations of the two **CD** molecules (confronting the **CDs** on both their HP-residues, and then rotating 180° each **CD** at a time, or both, models with letters A–D). The models for the **PL01-HP-β-CD** 1 : 1 type complex were also studied to confront with the other **CDs**, by including 250 molecules of H_2O this time, like in **β-** and **γ-CD**. For both systems, the model for the separate host and guest was also prepared and optimized. In summary, a total of 57 models were carried out for each different guest (**PL01** and **PL07**)–host (**β-**, **γ-** and **HP-β-CD**) system and the 5–-24 geometric possibilities. The mean calculation time was 20–30 days, depending on the number of atoms, on an average computer with an Intel Core i7-6900K CPU at 3.20 GHz, 3201 MHz, 8 core, 16 logic processors, using 64 GB RAM and running on Microsoft Windows 10 Enterprise.

Bioassays on parasitic weeds

Free **CDs**, **PL01**, **PL04** and **PL07** and their complexes were tested on the germination of seeds of *O. cumana*, *P. ramosa*, and *O. crenata* in the concentration range of 100–0.1 μM by following the previously reported method.[30]

Conclusions

The complexation of phthalimide-lactones with cyclodextrins allowed us to increase their solubility to different degrees depending on the presence of functional group(s) at the aro-

matic ring and the cyclodextrins employed. The best results were obtained with **PL01**, with an increase of water solubility almost 4 times.

The titration calorimetry employed in this study allowed us to verify the results with the experiment designed by Higuchi and Connors, but using a significantly smaller amount of the sample and experiment time, thus determining correctly the stoichiometry of the complex **PL01-HP-β-CD** formed as 1 : 2. The molecular modelling supported theoretically the experimental results of the phase-solubility diagram, the solubility and the bioactivity experiments, thereby allowing us to explain and predict the behavior of phthalimide-lactones in water. In fact, the lowest energies were obtained for **PL-HP-β-CD** aggregates, which produced the most soluble complexes.

All the results above demonstrated that **β-CD** and its derivative **HP-β-CD** are the best choices amongst the studied **CDs** for the complexation of **PLs**. The bioactivity results demonstrated that without the addition of an organic co-solvent, similar levels of bioactivity can be achieved after treatment with cyclodextrins. This bioactivity can even be increased, as such was the case of **HP-β-CD**.

This work concludes that future studies on germination inducers chemically similar to these compounds should be carried out with these cyclodextrins or their derivatives. The use of cyclodextrins would allow us to maintain or even increase the bioactivity of germination inducers without using organic co-solvents as a greener and safer alternative to traditional preparations.

Author contributions

Conceptualization: A. C. P., F. J. R. M., J. A., and J. M. G. M.; data acquisition: A. C. P., F. J. R. M., and C. R.; data curation: A. C. P., F. J. R. M., J. A., and C. R.; writing—original draft preparation: A. C. P., F. J. R. M., and C. R.; writing—review and editing: A. C. P., F. J. R. M., J. A., C. R., J. M. G. M., J. A. A., S. S., and F. A. M.; supervision: J. M. G. M., and F. A. M.; funding acquisition: J. M. G. M., and F. A. M. All authors have read and agreed to the published version of the manuscript.

Conflicts of interest

There are no conflicts to declare.

Acknowledgements

This research was funded by the Spanish Agencia Estatal de Investigación (project PID2020-115747RB-I00). A. C. P. expresses his sincere gratitude for the financial support from the "Plan Propio—UCA 2022–2023", call "INVESTIGADORES NOVELES, Proyectos para impulsar su Carrera Científica" (Project PR2022-043); the "Consejería de Economía, Conocimiento, Empresas y Universidad de la Junta de Andalucía"; and the "Programa Operativo Fondo Social Europeo de Andalucía 2014–2020". F. J. R. M. thanks the University of Cádiz for the postdoctoral support with the Margarita Salas fellowship 2021-067/PN/MS-RECUAL/CD, funded by the NextGenerationEU programme of the European Union. The authors want to thank professors Leonardo Velasco (CSIC, Córdoba, Spain) and Maurizio Vurro (National Research Council – Institute of Sciences of Food Production, Bari, Italy) for kindly providing the seeds for the parasitic weed bioassays.

Notes and references

1 V. Gomez-Roldan, S. Fermas, P. B. Brewer, V. Puech-Pagès, E. A. Dun, J.-P. Pillot, F. Letisse, R. Matusova, S. Danoun, J.-C. Portais, H. Bouwmeester, G. Bécard, C. A. Beveridge, C. Rameau and S. F. Rochange, *Nature*, 2008, **455**, 189–194.
2 H. Liu, C. Li, M. Yan, Z. Zhao, P. Huang, L. Wei, X. Wu, C. Wang and W. Liao, *J. Plant Res.*, 2022, **135**, 337–350.
3 Q. Ma, X. Lin, M. Zhan, Z. Chen, H. Wang, F. Yao and J. Chen, *Int. J. Food Sci. Technol.*, 2022, **57**, 619–630.
4 D. Blanco-Ania and B. Zwanenburg, *Methods in Molecular Biology*, 2021, pp. 37–55.
5 X. Xie, K. Yoneyama and K. Yoneyama, *Annu. Rev. Phytopathol.*, 2010, **48**, 93–117.
6 C. Parker, *Pest Manage. Sci.*, 2009, **65**, 453–459.
7 F. J. R. Mejías, M. López-Haro, L. C. Gontard, A. Cala, M. Fernández-Aparicio, J. M. G. Molinillo, J. J. Calvino and F. A. Macías, *ACS Appl. Mater. Interfaces*, 2018, **10**, 2354–2359.
8 C. Rial, S. Tomé, R. M. Varela, J. M. G. Molinillo and F. A. Macías, *J. Chem. Ecol.*, 2020, **46**, 871–880.
9 R. G. Pereira, A. Cala, M. Fernández-Aparicio, J. M. G. Molinillo, M. A. D. Boaventura and F. A. Macías, *Pest Manage. Sci.*, 2017, **73**, 2529–2537.
10 X. Xie, D. Kusumoto, Y. Takeuchi, K. Yoneyama, Y. Yamada and K. Yoneyama, *J. Agric. Food Chem.*, 2007, **55**, 8067–8072.
11 F.-D. Boyer, A. de Saint Germain, J.-P. Pillot, J.-B. Pouvreau, V. X. Chen, S. Ramos, A. Stévenin, P. Simier, P. Delavault, J.-M. Beau and C. Rameau, *Plant Physiol.*, 2012, **159**, 1524–1544.
12 S. Li, Y. Li, L. Chen, C. Zhang, F. Wang, H. Li, M. Wang, Y. Wang, F. Nan, D. Xie and J. Yan, *Plant J.*, 2021, **107**, 67–76.
13 K. Fukui, D. Yamagami, S. Ito and T. Asami, *Front. Plant Sci.*, 2017, **8**, 936.
14 A. Hýlová, T. Pospíšil, L. Spíchal, J. J. Mateman, D. Blanco-Ania and B. Zwanenburg, *New Biotechnol.*, 2019, **48**, 76–82.
15 A. Cala, K. Ghooray, M. Fernández-Aparicio, J. M. G. Molinillo, J. C. G. Galindo, D. Rubiales and F. A. Macías, *Pest Manage. Sci.*, 2016, **72**, 2069–2081.
16 B. A. Kountche, M. Jamil, D. Yonli, M. P. Nikiema, D. Blanco-Ania, T. Asami, B. Zwanenburg and S. Al-Babili, *Plants, People, Planet*, 2019, **1**, 107–118.
17 E. M. M. Del Valle, *Process Biochem.*, 2004, **39**, 1033–1046.
18 J. Szejtli, *Chem. Rev.*, 1998, **98**, 1743–1753.

19 A. Moeini, M. Masi, M. C. Zonno, A. Boari, A. Cimmino, O. Tarallo, M. Vurro and A. Evidente, *Org. Biomol. Chem.*, 2019, **17**, 2508–2515.
20 A. Cala, J. M. G. Molinillo, M. Fernández-Aparicio, J. Ayuso, J. A. Álvarez, D. Rubiales and F. A. Macías, *Org. Biomol. Chem.*, 2017, **15**, 6500–6510.
21 S. S. Braga, *Biomolecules*, 2019, **9**, 801.
22 T. Higuchi and K. A. Connors, *Adv. Anal. Chem. Instrum.*, 1965, **4**, 117–212.
23 C. Schönbeck, T. L. Madsen, G. H. Peters, R. Holm and T. Loftsson, *Int. J. Pharm.*, 2017, **531**, 504–511.
24 P. Saokham, C. Muankaew, P. Jansook and T. Loftsson, *Molecules*, 2018, **23**, 1161.
25 W. Saenger, *Angew. Chem., Int. Ed. Engl.*, 1980, **19**, 344–362.
26 I. Ghosh and W. M. Nau, *Adv. Drug Delivery Rev.*, 2012, **64**, 764–783.
27 T. Loftsson and M. Másson, *J. Drug Delivery Sci. Technol.*, 2004, **14**, 35–43.
28 T. Loftsson and M. E. Brewster, *J. Pharm. Sci.*, 2012, **101**, 3019–3032.
29 C. M. Fernandes, R. A. Carvalho, S. Pereira da Costa and F. J. B. Veiga, *Eur. J. Pharm. Sci.*, 2003, **18**, 285–296.
30 J. G. Zorrilla, A. Cala, C. Rial, F. J. Francisco, J. M. G. Molinillo, R. M. Varela and F. A. Macías, *J. Agric. Food Chem.*, 2020, **68**, 9636–9645.
31 M. Fernández-Aparicio, X. Reboud and S. Gibot-Leclerc, *Front. Plant Sci.*, 2016, **7**, 135–151.
32 M. Pérez-Abril, C. Lucas-Abellán, J. Castillo-Sánchez, H. Pérez-Sánchez, J. P. Cerón-Carrasco, I. Fortea, J. A. Gabaldón and E. Núñez-Delicado, *J. Funct. Foods*, 2017, **36**, 122–131.